Compartmentalized Nanocomposite for Dynamic Nitric Oxide Release

ARTICLE *in* THE JOURNAL OF PHYSICAL CHEMISTRY B · DECEMBER 2008

Impact Factor: 3.3 · DOI: 10.1021/jp803276u · Source: PubMed

5 AUTHORS, INCLUDING:

Sabrina Jedlicka
Lehigh University
23 PUBLICATIONS **147** CITATIONS
SEE PROFILE

Jenna Rickus
Purdue University
51 PUBLICATIONS **667** CITATIONS
SEE PROFILE

Article

Compartmentalized Nanocomposite for Dynamic Nitric Oxide Release

John J. Koehler, Jianxiu Zhao, Sabrina S. Jedlicka, D. Marshall Porterfield, and Jenna L. Rickus

J. Phys. Chem. B, **2008**, 112 (47), 15086-15093 • Publication Date (Web): 01 November 2008

Compartmentalized Nanocomposite for Dynamic Nitric Oxide Release

John J. Koehler,[†,∥] Jianxiu Zhao,[†,∥] Sabrina S. Jedlicka,[†,∥,⊥] D. Marshall Porterfield,[†,‡,§,∥] and Jenna L. Rickus*[,†,§,∥]

Department of Agricultural and Biological Engineering, Department of Horticulture and Landscape Architecture, Weldon School of Biomedical Engineering, Physiological Sensing Facility at the Bindley Bioscience Center, Purdue University, West Lafayette, IN

Received: April 15, 2008; Revised Manuscript Received: August 8, 2008

Nitric oxide (NO) is an important cell-signaling molecule whose role in a variety of cellular processes such as differentiation and apoptosis depends strongly on its concentration and flux levels. This work describes and characterizes a novel nitric oxide releasing nanocomposite, capable of photostimulated NO flux that can by dynamically modulated in within a range of biological levels. This material mimics the common compartmentalization strategies used by living cells to achieve its novel features. The material is constructed by encapsulating a photosensitive nitric oxide donor within lipid vesicles with an average diameter of 150 nm. The vesicles are then doped into the interstitial liquid phase of a solid porous silica matrix, which has previously demonstrated biological compatibility and capabilities as a growth surface for mammalian cells. Stimulation by a light source produces a step increase in NO concentration within seconds. The NO flux at the surface of the material is measured to be 14 pmol-cm^{-2} sec^{-1} using a NO selective self-referencing amperometric microsensor. The NO concentration profile decreases with distance perpendicular to the surface as expected for diffusion from a surface through an aqueous environment. A pattern of one minute light pulses produced uniform pulses of increased NO concentration of one minute duration. A linear relationship exists between NO surface concentration and photon flux, and this relationship can be used to tune the material response.

Introduction

Cell to cell communication is dynamic and responsive. Biomaterials that mimic natural signaling for cell and tissue manipulation also need to be dynamic and responsive. The spatial and temporal control of biological properties and signals at the material-cell interface is therefore a current challenge in biointerface science.[1] Some notable materials have utilized electrical,[2,3] mechanical,[4] thermal,[5] and photochemical events to create dynamic surfaces to influence cell processes.[6] These materials mainly focus on the manipulation of material surface properties [7,8] for controlling cell adhesion.[5,9] Extracellular signals that modulate cell processes such as differentiation include not only nondiffusible contact cues but also diffusible chemical cues. Material surfaces capable of temporally and spatially controlled flux of diffusible signals are, therefore, also needed.

Nitric oxide (NO) is a unique cellular signaling molecule that functions in a diverse range of cellular processes[10] including bone remodeling,[11] neuronal differentiation,[12] and apoptosis.[13] NO is produced by intracellular enzymes, but can permeate cell membranes[14] to reach extracellular spaces and adjacent cells. In addition, NO typically has a short half-life (seconds) in tissues[15] allowing the molecule to act as a local cell−cell communication signal. In addition, the effects of NO are highly concentration or flux dependent creating a complex role for the molecule in opposing processes such as neural protection and neural degeneration.[16,17] Material surfaces capable of delivering a range of controlled NO flux to cells would enable a useful experimental paradigm for elucidating the function of NO. In addition, NO releasing materials have application in modulating the biocompatibility of biosensors[18] and biomedical implants.

In this work, we present a novel biologically and chemically doped porous nanocomposite material[19] that is produced using sol−gel synthesis methods and is capable of delivering a range of biologically relevant and temporally controlled NO flux from a single sample. The material mimics the cellular compartmentalization of membrane impermeable NO donors along with the intracompartmental production and trans-compartmental release of membrane permeable NO (Figure 1). The photosensitive NO donor, *S*-nitroso-*N*-acetylpenicillamine (SNAP), is encapsulated inside large unilamellar vesicles (LUV), also known as liposomes, which are in turn doped within porous silica by a sol−gel synthesis method. The liposomes serve as an artificial cell membrane that prevents the leaching of the NO donor. The porous silica provides a solid state environment to serve as a cellular substrate[20,21] or device coating and to prevent the uptake of the liposome nanoparticles by cells at the surface. In addition, the porous silica increases the stability of the liposomes by preventing aggregation.[22] Previously we showed that liposomes in a sol−gel silica environment matrix are stable for many months.[23,24]

Schoenfisch et al. has developed sol−gel methods to produce NO releasing materials[25] with applications that include protective coatings for implanted devices to limit microbial activity,[26−28] or decreasing platelet adhesion.[29−31] The NO donors in these materials are conjugated to the silica matrix resulting in a material with a high mass fraction of NO,[32,33] but the initiation

* To whom correspondence should be addressed. E-mail: rickus@purdue.edu. Phone: (765)494-1197. Fax: (765) 496-1115.
† Department of Agricultural and Biological Engineering.
‡ Department of Horticulture and Landscape Architecture.
§ Weldon School of Biomedical Engineering.
∥ Physiological Sensing Facility at the Bindley Bioscience Center.
⊥ Current Affiliation: Department of Materials Science and Engineering, Lehigh University, Bethlehem, Pennsylvania 18015.

10.1021/jp803276u CCC: $40.75
Published on Web 11/01/2008

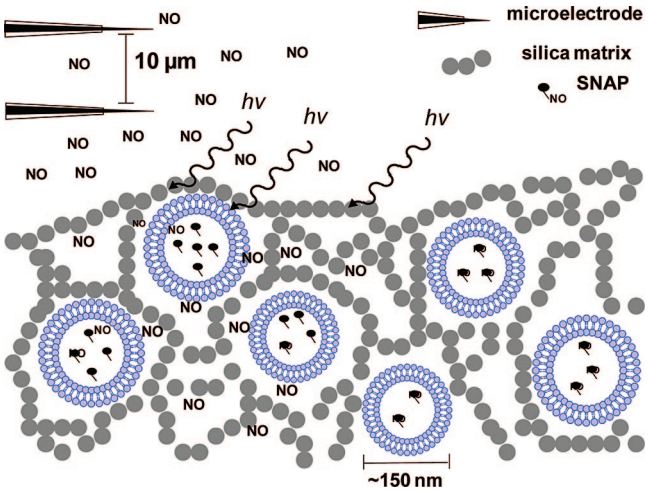

Figure 1. Compartmentalized nanocomposite material for light controlled nitric oxide release. In the dark NO is bound in the donor molecule, SNAP, which cannot diffuse through the liposome compartment membrane. The liposome is trapped within pores of the silica cell culture substrate. Upon exposure to light the SNAP controllably releases NO, which diffuses to the surface of the material.

and magnitude of NO release is spontaneous in physiological conditions. In addition the NO flux is controllable by the material composition but is not controllable after the material is assembled. These features are ideal for implant applications requiring continuous release but are undesirable for cell signaling applications where a dynamic modulation of the flux magnitude is desired. The material we present is distinct in that the NO release is controllable on a time scale of seconds with a potential to change the temporal patterns of release by changing the light stimulation intensity and pattern.

Frost et al. also used the NO donor, SNAP, along with nonsol−gel methods to create a photocontrollable NO releasing polymer from SNAP-coated nanoparticles.[34,35] Because reducing agents such as copper, iron, and ascorbic acid can also catalyze NO release from SNAP,[15] a hydrophobic protective polymer coating was necessary in these materials for use in biological systems. The protective film decreased material performance between 5−35% of the initial flux.[36] In addition the hydrophobic polymer would be undesirable as cell culture surface. In the presented material design, a lipid bilayer creates nanothin protective barrier (∼3−5 nm thickness)[37] around the SNAP molecules that is easily permeated by the NO, eliminating the external protective coating at the cell-material interface. The sol−gel matrix support remains at the surface and has been shown to be able to support mammalian cell growth.[38−40]

The presented materials allow new biological experimental paradigms for dynamic NO modulation in culture systems. For example, the materials could be used in a closed-loop experimental setup[41] along with a NO microsensor and a controllable light source. The NO sensor would provide continuous feedback regarding NO flux at the surface of the material, such that the light source would be adjusted dynamically to either clamp the NO at a particular level or to produce a particular temporal pattern of NO flux. Such a system does not require the precise reproducibility between different batches of material surfaces by allowing for an internal calibration of the materials during each experiment. What is required is that changing the photon flux to the surface can modulate the NO flux both up and down. In addition the materials must be able to generate NO fluxes within the range of biological significance. We demonstrate these material features in this work using an open-loop system. The open-loop system provides a predetermined light pattern (either constant or step functions) and measures the NO flux and concentration at the surface of the material using an NO microsensor.

Experimental Methods

Materials Preparation. Tetramethoxysilane (TMOS), dihexadecyl hydrogen phosphate, ferric chloride hexahydrate, and ammonium thiocyanite were purchased from Fluka. 1,2-Dimyristoyl-*sn*-glycero-3-phosphocholine (DMPC) and cholesterol were purchased from Avanti Polar Lipids. *S*-nitroso-*N*-acetylpenicillamine (SNAP) was purchased from Invitrogen. Calcein was purchased from MP Biomedicals. The sephadex G-50 fine was obtained from Pharmacia. The ionic detergent, Triton X-100, and nafion were purchased from Sigma-Aldrich. Chloroform was purchased from Mallinckrodt. *O*-phenylenediamine (o-PD) was purchased from Wako. Phosphate buffered saline (PBS) was obtained from HyClone. Gaseous nitric oxide (NO) was purchased for People's Welding Supply in West Lafayette, Indiana.

Liposome vesicles were produced as previously published[24] with minor modification. The lipid stock solution consists of DMPC, cholesterol, and dihexadecyl hydrogen phosphate at a 5:4:1 molar ratio dissolved in chloroform. A thin lipid film was formed on the walls of a glass vial and 2 mM SNAP solution in 0.02 M pH 6.0 phosphate buffer with 1 μM EDTA was added. The lipid film was vortexed for 10 min and allowed to rest for 30 min before extrusion using a miniextruder (Avanti Plar Lipids) with two 1 mL gastight Hamilton syringes and a 100 nm pore size polycarbonate filter (Whatman). The average vesicle diameter was measured to be 150 nm with a standard deviation of 83 nm by dynamic light scattering (Supporting Information).

Liposomes were purified from free SNAP in solution through a variation of the minicolumn method.[42] The minicolumn method was selected to produce liposome solutions at the highest possible concentration while avoiding liposome agglomeration in solution. Minicolumns were produced by fitting the barrel of a 5 mL syringe filled with sephadex into a 15 mL centrifuge tube. Excess buffer was removed by spinning the minicolumn twice for three minutes at 400 g. Liposome purification was achieved by slowly adding up to 250 μL of liposome solution to the top of the sephadex pellet, then spinning the columns at 400 g for 4 min.

TMOS (3.8 mL), sterile 18 MΩ-cm water (0.85 mL) and 0.04 M HCl (55 μL) was sonicated in a water bath sonicator at room temperature for 15 min, or until the mixture appeared homogeneous. If the liquid sol appeared cloudy, it was filtered through a Whatman syringe filter with 0.2 μm pore size. Methanol was removed by rotary evaporation with a Buchi 200 at 337 mbar and 40 °C after dilution 2:3 by volume with sterile 18 MΩ-cm water. The liquid sol was stored in the freezer for 24 h before use. Bulk gels were formed by mixing the liquid TMOS sol with liposome vesicle solution 40%−60% by volume. The bulk gels were covered in 0.02 M pH 6.0 phosphate buffer and stored at 8 °C prior to use.

The compartmental materials were previously characterized using cryo-SEM and TEM.[43] Cryo-SEM characterized the surface of the materials and confirmed the amorphous morphology and mesoporosity of the silica, but the embedded liposomes could not be visualized using this technique. Freeze-fracture TEM using negative staining, a sample preparation method optimized for biomolecule embedded matrices, confirmed the relative liposome size and the preservation of the liposome

membrane within the material pores. Conclusive information regarding the spatial distribution of the liposomes throughout the matrix could not be obtained from this technique due to sampling limitations of the method.

An additional consideration for use in cellular systems is that acidic conditions can also induce NO release from SNAP.[41] Cells may create local changes in pH if significant cellular fluxes of protons or lactic acid are present. Characterization using pH sensitive dyes within the liposomes indicates that pH changes at the surface of the material are slow to translate into changes in pH inside the liposomes in the materials (data not shown). In a well-buffered system, we do not expect such effects to create significant NO leak, although this should be explicitly examined for any particular cell system.

SNAP Dissociation Kinetics Within the Material by Spectrophotometry. The kinetics of SNAP dissociation were followed using UV absorbance at 337 nm. A dilution series of SNAP in 100 μL sol−gel topped with 100 μL of 0.02 M pH 6.0 phosphate buffer with 1 μM EDTA was used to create a calibration curve. Bulk gels were formed in individual wells of a UV-transparent 96 well plate. Measurements were repeated in triplicate and linear regression was preformed on the average absorbance at each concentration.

TMOS gels with an approximate SNAP concentration of 12 mM were prepared as described above. Half of the gels were exposed to a 100 W light source, while the other half of the gels were protected from light. The absorbance was measured every 20 min until absorbance measurements for the excited gels stabilized. The kinetics were measured simultaneously for four different samples and regression was performed independently to measure the release rate coefficient for each sample. The procedure was repeated for SNAP in phosphate buffer.

Vesicle Characterization. The encapsulation volume was measured using a calcein fluorescence assay. A calcein dilution series with concentrations from 0−40 μM was used to construct a calibration curve. All calcein fluorescence measurements were taken using a Fluoromax with MicroMax 96 well plate reader (Jobin Yvon) with λ_{ex} of 485 nm and λ_{em} of 535 nm. Four replicates were taken at each concentration and regression analysis was preformed on the average fluorescence intensity at each concentration.

Liposomes used in the assay were produced by the method described above, but 2 mM SNAP was replaced by 50 mM calcein in 0.02 M pH 6.0 phosphate buffer. At this concentration, the calcein fluorescence is self-quenched. Liposomes were ruptured using 10% (vol %) Triton-X100 in water. Fluorescence intensity measurements were taken before Triton addition and 15 min after Triton addition, and the relative increase in fluorescence intensity was recorded. Four replicates were taken for each liposome solution and the average fluorescence intensity was used in encapsulation volume calculations.

Phospholipid concentration was measured using the colorimetric method.[44] A stock solution of ammonium ferrothiocyanate was produced by dissolving 27.03 g ferric chloride hexahydrate ($FeCl_3 6H_2O$) and 30.4 g ammonium thiocyanite (NH_4SCN) in 1 L of sterile 18 MΩ water. A standard calibration curve for phospholipid concentration was constructed. Each phospholipid sample was vigorously mixed with an equal volume of salt solution for one minute. The organic phase was separated from the aqueous phase using a glass pipet. The absorbance was scanned between 350−550 nm using a SpectraMax Plus384 (Molecular Devices). All lipid concentrations were done in triplicate, and the average values are plotted and linear regression analysis was preformed to fit the calibration curve.

To measure phospholipid concentration of liposomes, an aliquot of liposomes in aqueous solution was dried on the walls of a screw cap vial under a stream of dry nitrogen. The lipid film was dissolved in chloroform by vigorously mixing for several minutes. The sample was divided into thirds and each aliquot was analyzed for lipid content by the same method as the lipid standard solution. The three measurements were averaged when calculating the phospholipid concentration.

Self-Referencing Amperometric NO Microsensor. NO sensitive microelectrodes were prepared and calibrated based on previously described procedures.[45] Bare carbon fiber electrodes were purchased from Kation Scientific. After coating with Nafion and o-PD, the electrode has been shown to have specific sensitivity toward NO with a selectivity of 600:1 for ascorbic acid, 900:1 for nitrite.[46] The previously measured detection limit, defined by a 3:1 signal-to-noise ratio, for the coated electrode is 35 ± 7 nM NO.[46] Electrodes were coated in Nafion (5% in aliphatic alcohols) by dipping the recording end of the electrode in Nafion then drying at 110 °C for 10−15 min. Electrodes were electroplated in a solution of 5 mM o-PD and 0.1 mM ascorbic acid in 100 mM phosphate buffered saline (PBS). The o-PD solution was prepared fresh for each use and plated on the electrode at a potential of +900 mV until a stable current was obtained.[45,47] The probes were stored dry between experiments.

To calibrate the microsensor, a stock solution of 2 mM NO was created by bubbling dry argon through an airtight container of sterile 18 MΩ water for 30 min, then bubbling gaseous NO through the argon-purged water. The electrode tip was immersed in a 35 mm diameter Petri dish containing 5 mL of PBS. An airtight syringe (Chemglass) was used to withdraw a small volume of NO stock solution and add the stock solution to the PBS in the Petri dish. The contents of the Petri dish were rapidly mixed to equilibrate the solution. NO concentration measurements were taken with the electrode polarized to +900 mV. As soon as the signal from the electrode stabilized, more NO stock was added to the Petri dish. The average signal was recorded every 0.25 s and several recordings were taken at each concentration to create the calibration curve. The average and standard deviations were plotted and linear regression analysis performed to find the calibration curve. To account for intra and intersensor variability, each electrode was calibrated before and after each experiment.

The sensor was operated in self-referencing mode for NO flux measurements and was calibrated using a NO point source, based on previously described methods.[47] The point source was constructed by pulling a micropipette down to a 5 μm opening, then backfilling the micropipette with 0.5% by mass agar with 2 mM SNAP in sterile 18 MΩ water. The electrode was polarized to +900 mV, and self-referencing mode NO flux measurements were made using a 10 μm excursion moving at a frequency of 0.3 Hz. The electrode was moved within the artificial gradient, away from the point source as the experiment progressed using step sizes of 2, 5 μm, and 10 μm. Concentration was measured using only the signal at the probe origin, while flux was calculated using the differential signal. At each probe location, between 10 and 20 measurements were recorded and the average flux and concentration was plotted with error bars representing the standard deviation.

Material Surface NO Flux Measurements by the NO Microsensor. Surface flux measurements of NO under different photostimulation conditions were recorded using a single, NO-

selective microelectrode placed at the top surface of the material. Flux and concentration measurements were obtained above the surface of the material by moving the probe tip using the computer-controlled stepper motor interface. For flux measurements, the electrode was operated in a self-referencing mode.[47] This approach measures flux, based on Fick's Law, using a single sensor which is oscillated (frequency of 0.3 Hz) between two distinct locations (10 μm apart) within a diffusional gradient. The linear path of the microelectrode was tangent to the surface with the closest point within 1−2 μm of the surface. For step-back experiments, the probe was moved away from the surface using step sizes of either 2 or 5 μm, with a 2 μm step used near the surface and a 5 μm step sized used as the distance from the surface increased.

Bulk gels of 1 mm thickness with immobilized liposomes were used for all NO measurements from the material surface. The sol−gel was topped with buffer as soon as gelation occurred and condensation was allowed to continue for 24 h before using the gel. The large bulk gel was broken into smaller pieces so several measurements could be made with the same material to reduce batch-to-batch variation. The material was covered with PBS with 1 μM EDTA during measurements.

During microsensor measurements the gels were placed in a clear open tissue culture plate and excited from above using a broad spectrum light source. The microelectrode sensors were placed on the top surface as well. The light source and electrode were angled such that the electrode did not shield the materials from the light path. The photon flux from the light source was measured with a GMSW-SS quantum meter (Apogee Instruments) placed at the material surface. On average 10 to 20 recordings were taken at each location and the average and standard deviation were plotted for analysis.

Results and Discussion

NO Production Kinetics. The decay of the S−N bond of SNAP and subsequent NO release upon light excitation was measured by spectrophotometry. Decay rates for SNAP-doped gels were estimated and compared to that of SNAP in solution. In solution SNAP has a peak absorbance at 335 nm and an expected molar extinction coefficient of 519 $M^{-1}cm^{-1}$ [15]. A dilution series of SNAP doped silica monoliths (i.e., bulk materials with a thickness of 1 mm) produced a linear calibration of SNAP concentration with a peak absorbance at 337 nm and an experimentally measured molar extinction coefficient of 499 $M^{-1}cm^{-1}$. Upon excitation SNAP-doped gels demonstrated an exponential decay with a first order rate constant of -0.029 ± 0.00081 min^{-1} (Figure 2A). This dissociation rate was more than twenty times greater than the spontaneous SNAP dissociation rate in the dark. The generation rate of NO from SNAP in phosphate buffer under the same light excitation conditions was of a similar order of magnitude, -0.050 $min^{-1} \pm 0.0058$ (Figure 2B).

The rates of chemical reactions conducted within the pores of sol−gel produced materials can be an order of magnitude slower compared to the same reaction conducted in a well-mixed solution.[48−51] This difference is often attributed to diffusion limitations or multiple populations of molecules in different regions of the porous matrix. In this case the photochemical production of NO from SNAP is not dependent on bimolecular collisions and should not be reduced by diffusion limitations. The small decrease in the decay rate for SNAP in solution compared the gel could be due to interactions between the matrix pore walls and subpopulations of the SNAP molecules.

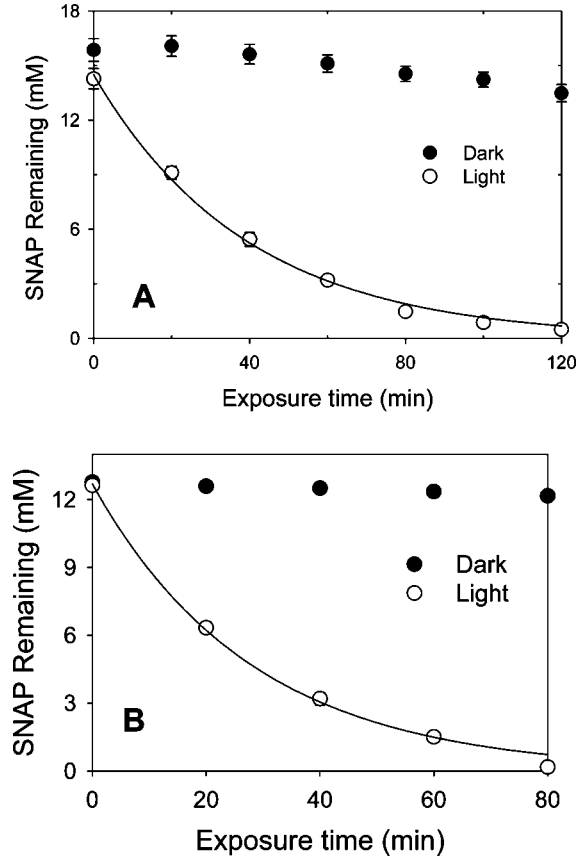

Figure 2. SNAP retains light sensitivity inside the porous silica. (A) The decomposition of SNAP in the silica after exposure to light follows a first order exponential decay with a rate constant of 0.029 ± 0.00081 min^{-1}. (B) The decomposition of SNAP in phosphate buffer has a first order decay rate constant of 0.050 ± 0.0058. These NO generation rates are over 20 times faster then SNAP in the dark. The average NO generation rate was calculated from the results of regression analysis on four sets of data and the error bars represent the standard error of the mean.

Liposome Encapsulation Efficiency. The bulk concentration of SNAP present in the material determines the overall NO production capacity and depends on the number of vesicles in the sol−gel as well as the number of SNAP molecules within each vesicle. The encapsulation efficiency of the liposomes, defined as the μL of encapsulated volume per μmol of lipid,[52] was calculated using experimental measurements of the liposome encapsulation volume and the total lipid concentration of the liposome solution.

Using calcein encapsulated liposomes and a linear calibration of calcein fluorescence as a function of concentration, the liposome encapsulation volume was measured to be 0.077 ± 0.0028 μL encapsulated volume per 100 μL liposome solution. Four independent liposome samples were used for the average and the reported interval is the standard error of the mean. The lipid concentration calibration curve showed a strong linear relationship between phospholipid concentration and absorbance at 466 nm. The lipid concentration in the liposome solution was measured to be 0.3 mg/mL using the same liposome solution as the encapsulation volume assay. Only 30% of the initial lipid concentration is recovered after liposome preparation, and further testing revealed that most of the lipid concentration is lost during the purification step.

The encapsulation efficiency for the liposome solution was 19.7 μL/μmol lipids using a 100 μL basis of liposome solution. The concentration of SNAP encapsulated by liposomes in the

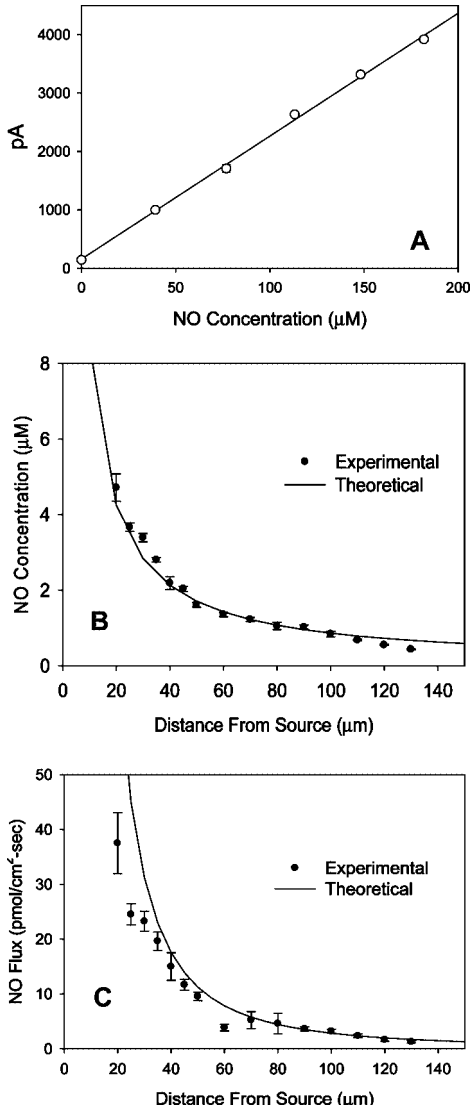

Figure 3. (A) A typical electrode has a linear response to NO concentration. Each point represents the average of 15−30 measurements at each concentration and the error bars represent the standard deviation. (B) Experimental NO concentration and (C) experimental NO flux values match the analytical solution for flux and concentration from a point source. Ten to fifteen data points were obtained for each point and the error bars represent the standard deviation.

nanocomposite material is equivalent to a material with a bulk SNAP concentration of 35 nM. Biological NO flux is commonly in the low pmol/cm^{-2} s^{-1} range[45,53] and higher fluxes are potentially cytotoxic.[54] A nanomolar SNAP concentration should therefore be sufficient for generating biologically relevant NO flux for short time durations.

NO Microelectrode Calibration and Validation from an Ideal Source. Calibration of the amperometric NO microsensors resulted in a linear relationship between output signal in pA to NO concentration (Figure 3A) with the response ranging from 10−35 pA per μM change in NO concentration. Individual electrodes displayed different characteristic responses and Figure 3 shows a typical response curve for one electrode. To compensate for interelectrode variability, each electrode was calibrated before and after each experiment. The resulting calibrations were used to analyze raw data taken from the matched electrode only.

To validate the microsensor calibration, NO flux measurements were compared for accuracy against known flux artificial

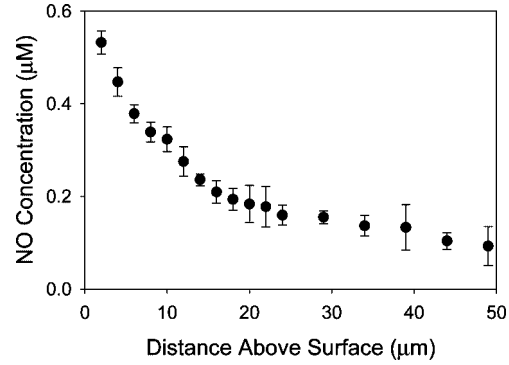

Figure 4. Photostimulation creates a stable NO gradient in a direction perpendicular to the surface. The NO flux at the surface was calculated to be 14.0 pmol cm^{-2} sec^{-1}. Each data point represents the average of ten to twenty measurements taken at each position above the surface. The error bars represent the standard deviation.

source. A micropipette with a 5 μm opening was used to create an ideal point source of NO. The concentration gradient away from this source can modeled theoretically as previously described[45]

$$C(r) = \left(\frac{C_0 R_0}{r}\right) e^{\left[\frac{-(r - R_0)^2 k}{2D}\right]} \quad (1)$$

where C_0 is the NO concentration at the source, previously determined to be 17 μM for 2 mM SNAP in 0.5% agar,[45] and R_0 is the radius of the point source. The diffusion coefficient, D, for NO in water is 3.3 × 10^{-5} cm^2 s^{-1} at 37 °C. The rate constant for NO destruction in solution, k, is 0.012 s^{-1}.[45]

The NO flux in is then calculated using Fick's Law[45]

$$J = -D\frac{\Delta C}{\Delta r} \quad (2)$$

For the analytical case, the approximate derivative was replaced by the derivative of the NO concentration equation. The approximate derivative was calculated for the experimental case using the differential signal obtained from the self-referencing microsensor.

Figure 3B,C demonstrates that the experimental measurements for NO concentration and flux agree with the analytical solution for this simulation. Because of the inevitable exposure of the calibration point-source to light during the set up of the experiment, the initial NO concentration is below the 17 μM used in the theoretical solution. This causes both the experimental NO concentration and experimental NO flux to be consistently lower than the expected theoretical values. On the basis of these results, it is expected that the liposome-doped sol−gel will also release NO when exposed to ambient light. Therefore, exposure to ambient light must be minimized when preparing and handling the material to avoid unwanted release of NO and maximize the NO releasing potential of the surface. Given the short lifetime of NO in biological media, the released NO will dissipate within a reasonable time. A short rest period in the dark, after sample preparation and setup, allows any unwanted NO to dissipate before the experiment begins.

NO Release Under Constant Photostimulation. The results of NO concentration measurements at the material surface show the characteristic decay expected for diffusion from a plane source with degradation of products (Figure 4). From the concentration data the NO flux is calculated to be 14 pmol cm^{-2}

sec^{-1} at the surface, which is in the range of biological relevance. For comparison, individual macrophages in culture produce NO fluxes of ~1 pmol cm^{-2} sec^{-1}, while aggregates of 18−48 macrophages produce NO fluxes of 4−10 pmol cm^{-2} sec^{-1}.[45] NO surface fluxes of 30 pmol cm^{-2} sec^{-1} almost completely inhibit bacterial adhesion to surfaces indicating that this value is in the high range where destructive cellular mechanisms, such as membrane and DNA damage, occur.[55]

The theoretical maximum yield for encapsulated SNAP in immobilized liposomes is 35 nM as determined through the encapsulation efficiency. The NO concentration measured at a distance of 2 μm above the surface of the material is 532 nM, an order of magnitude higher than the theoretical maximum. Because the NO concentration at the surface of the material is greater than theoretical maximum SNAP concentration, but much less than the 2 mM SNAP solution used to make the liposomes, it is speculated that the difference between experimental and theoretical concentrations is caused by an incomplete separation of unencapsulated SNAP from liposomes encapsulating SNAP during the chromatography purification step. To correct for this problem of free SNAP, the materials were soaked in excess buffer for 24 h before use for all of the remaining experiments. In this way the porous silica matrix essentially acts as a second size separation step to remove the free SNAP while maintaining the liposomes.

To test the photosensitive nature of the NO releasing material, a light source was used to excite NO release while taking amperometric measurements above the surface of the material. The material was soaked in buffer for at least 24 h before the experiment to allow any unencapsulated SNAP to leach out of the glass matrix. Before stimulating the material, the sol−gel was allowed to equilibrate in the dark for thirty minutes to allow for the complete reaction of any NO released while preparing the sample. The light source was then held at a constant intensity until the end of the experiment.

The results of the photostimulated NO release experiments show an increase in NO concentration at the surface of the material. By analyzing the raw electrode output signal we note that there is a noticeable increase in signal within 12 s of stimulation (Figure 5A). Given the signal is linearly related to NO concentration, we can conclude that this increase is a release of NO. The immediate increase in NO concentration demonstrates that NO diffusion is not significantly inhibited by the liposome membrane or sol−gel structure. The liposomes might even facilitate NO diffusion in the material given NO diffusion in lipids is significantly faster that diffusion in water.[56]

NO Release in Response to Pulsed Light Stimulation. A shorter pulsed excitation was used to further analyze the kinetics and to demonstrate that NO flux can be repeatedly initiated in one sample of material. After allowing the material to equilibrate, the light source was pulsed for 1 min followed by a 15 min resting period. The intensity of the pulse was varied between 75 and 125 W, but the pulse at 75 W did not generate a detectible NO pulse. The two 1 min 125 W pulses generated uniform 36 nM spikes in NO concentration. This concentration is in agreement with the theoretical maximum predicted by the measured encapsulation efficiency. The duration of the NO spikes was equal the duration of the stimulation (Figure 5B).

In order to further demonstrate the dynamic properties of the material, the light intensity was stepped up to 75, 100, and 125 W, then stepped back down to zero excitation. As the excitation intensity was increased, the material responded with an incremental increase in NO concentration within 30 s of the excitation (Figure 6A). With 75 W excitation power there is no significant peak in NO release, but the background drift of the signal is halted. This is a positive sign that NO is being released at a concentration below the detection limit for the microsensor. When the intensity is stepped to 100 W there is a 12 nM increase

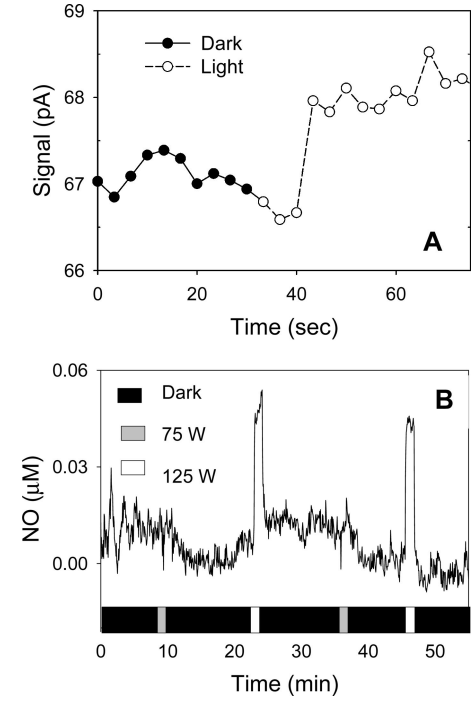

Figure 5. (A) Material response to stimulation with a 100 W light source. There is a rapid increase in NO concentration at the material surface within seconds after exposure. (B) Pulses from a 125 W light source create corresponding 36 nM pulses of NO from the material. Pulses from a 75 W light source do not generate a detectible amount of NO.

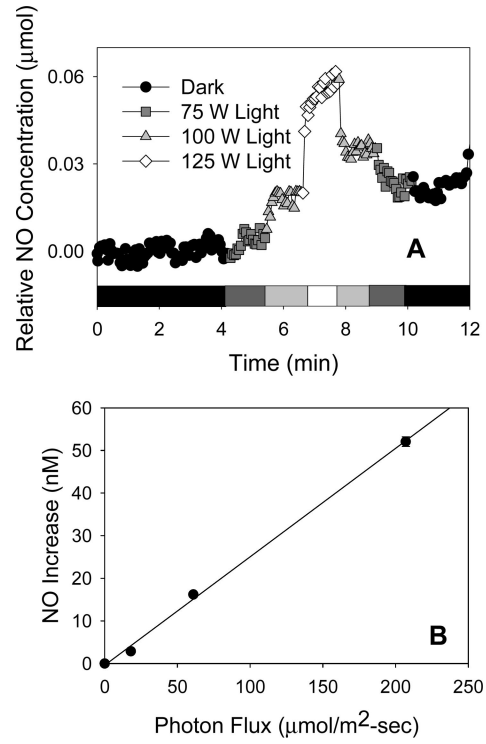

Figure 6. NO concentration is controlled by light intensity. (A) NO concentration at the surface of the sol−gel is dependent on the intensity of the stimulation source. (B) NO concentration above the surface increases linearly with photon flux through the material.

in NO concentration over a period of 12 s, and an increase in intensity up to 125 W results in a 29 nM increase in NO concentration over 9 s. When the intensity was stepped back down to 100 W there was a 21 nM decrease in NO concentration over a period of 24 s, and the NO concentration decreases by 11 nM over 12 s when the intensity returned to 75 W. The total increase in NO concentration while increasing the light intensity is 41 nM, but the NO concentration decreases by only 32 nM while decreasing the light intensity. This discrepancy may be caused by a buildup of NO at the material surface as the dissolved oxygen in and around the material surface is depleted. Alternatively, the failure of the signal to return to baseline after stimulation may also reflect the inherent drift in background signal in the microelectrode in concentration mode over long periods of time. This complication makes assessment of the complete reversibility of the material difficult and indicates that for long-term biological experiments, self-referencing measurements would be required.

Different excitation intensities lead to different NO concentrations at the surface of the nanocomposite, so calibration of the excitation level to produce a predictable NO concentration should be possible. In order to calibrate the amount of NO released against the exposure intensity, the flux of photons reaching the material surface was measured. The relationship between photon flux and NO concentration is linear as determined through regression analysis (Figure 6B). The equation describing the correlation between photon flux and NO concentration is:

$$[\mathrm{NO}] = 0.255(\mathrm{flux}) - 0.4189 \qquad (3)$$

where [NO] is the NO concentration in nM and flux is the photon flux in mmol cm^{-2} s^{-1}. Using this calibration method, it is possible to tune the NO concentration at the surface of the material by adjusting the intensity of the excitation source.

Conclusion

The research presented in this paper details the construction and characterization of a novel NO releasing material. The material consists of 2 mM SNAP encapsulated in liposomes of 150 nm diameter, which are then immobilized in a TMOS sol−gel matrix. Under these preparation conditions the bulk SNAP concentration is estimated at 35 nM, and the photosensitive properties of the nitric oxide donor are conserved. When stimulated by a light source the material releases a steady exponential gradient of NO moving away from the surface as measured by a self-referencing amperometric electrode. The NO flux at the surface is calculated from concentration measurements to be 14 pmol cm^{-2} sec^{-1}, which is potentially a biologically active flux. The release of NO is activated by exposing the material to light and exposure results in an almost instantaneous increase in NO concentration at the surface within twelve seconds of stimulation. The NO flux from the surface is dynamically responsive to stimulus from a light source, with a pattern of pulsed light signals producing a corresponding pattern of uniform NO pulses. When the excitation intensity is stepped up to 125 W, then stepped back down there is an incremental response in NO concentration at the surface of the material. With this controllability, it is possible to calibrate the material to release NO at a desired concentration, and there is a positive linear relationship between photon flux and amount of NO released.

Acknowledgment. The authors are grateful to funding from the USDA Nanotechnology National Research Initiative (Grant 102078), the Purdue University Agricultural Research Programs, and Purdue Research Foundation.

Supporting Information Available: Histograms for the dynamic light scattering measurement of liposome diameter. This material is available free of charge via the Internet at http://pubs.acs.org.

References and Notes

(1) Chilkoti, A.; Hubbell, J. A. *MRS Bull.* **2005**, *30*, 175.
(2) Lahann, J.; Mitragotri, S.; Tran, T. N.; Kaido, H.; Sundaram, J.; Choi, I. S.; Hoffer, S.; Somorjai, G. A.; Langer, R. *Science* **2003**, *299*, 371.
(3) Yeo, W. S.; Mrksich, M. *Langmuir* **2006**, *22*, 10816.
(4) Zhu, X. Y.; Mills, K. L.; Peters, P. R.; Bahng, J. H.; Liu, E. H.; Shim, J.; Naruse, K.; Csete, M. E.; Thouless, M. D.; Takayama, S. *Nat. Mater.* **2005**, *4*, 403.
(5) Yang, J.; Yamato, M.; Okano, T. *MRS Bull.* **2005**, *30*, 189.
(6) Mrksich, M. *MRS Bull.* **2005**, *30*, 180.
(7) Lahann, J.; Mitragotri, S.; Tran, T.-N.; Kaido, H.; Sundaram, J.; Choi, I. S.; Hoffer, S.; Somorjai, G. A.; Langer, R. *Science* **2003**, *299*, 371.
(8) Peng, D. K.; Yu, S. T.; Alberts, D. J.; Lahann, J. *Langmuir* **2007**, *23*, 297.
(9) Lahann, J.; Langer, R. *MRS Bull.* **2005**, *30*, 185.
(10) Murad, F. *Biosci. Rep.* **2004**, *24*, 452.
(11) Chow, J. W. M.; Fox, S. W.; Lean, J. M.; Chambers, T. J. *J. Bone Miner. Res.* **1998**, *13*, 1039.
(12) Peunova, N.; Enikolopov, G. *Nature* **1995**, *375*, 68.
(13) Albina, J. E.; Cui, S. J.; Mateo, R. B.; Reichner, J. S. *J. Immunol.* **1993**, *150*, 5080.
(14) Subczynski, W. K.; Lomnicka, M.; Hyde, J. S. *Free Radical Res.* **1996**, *24*, 343.
(15) Feelisch, M.; Stamler, J. S. *Methods in Nitric Oxide Research*; John Wiley & sons Ltd: New York, 1996.
(16) Blaise, G. A.; Gauvin, D.; Gangal, M.; Authier, S. *Toxicology* **2005**, *208*, 177.
(17) Bishop, A.; Anderson, J. E. *Toxicology* **2005**, *208*, 193.
(18) Gifford, R.; Batchelor, M. M.; Lee, Y.; Gokulrangan, G.; Meyerhoff, M. E.; Wilson, G. S. *J. Biomed. Mater. Res., Part A* **2005**, *75A*, 755.
(19) Gill, I. *Chem. Mater.* **2001**, *13*, 3404.
(20) Zolkov, C.; Avnir, D.; Armon, R. *J. Mater. Chem.* **2004**, *14*, 2200.
(21) Jedlicka, S. S.; McKenzie, J. L.; Leavesley, S. J.; Little, K. M.; Webster, T. J.; Robinson, J. P.; Nivens, D. E.; Rickus, J. L. *J. Mater. Chem.* **2006**, *16*, 3221.
(22) Zhao, J.; Jedlicka, S.; Lannu, J.; Bhunia, A. K.; Rickus, J. L. *Biotechnol. Prog.* **2006**, *22*, 32.
(23) Besanger, T.; Zhang, Y.; Brennan, J. D. *J. Phys. Chem. B* **2002**, *106*, 10535.
(24) Zhao, J. X.; Jedlicka, S. S.; Lannu, J. D.; Bhunia, A. K.; Rickus, J. L. *Biotechnol. Prog.* **2006**, *22*, 32.
(25) Shin, J. H.; Metzger, S. K.; Schoenfisch, M. H. *J. Am. Chem. Soc.* **2007**, *129*, 4612.
(26) Nablo, B. J.; Rothrock, A. R.; Schoenfisch, M. H. *Biomaterials* **2005**, *26*, 917.
(27) Nablo, B. J.; Chen, T. Y.; Schoenfisch, M. H. *J. Am. Chem. Soc.* **2001**, *123*, 9712.
(28) Hetrick, E. M.; Schoenfisch, M. H. *Biomaterials* **2007**, *28*, 1948.
(29) Frost, M. C.; Reynolds, M. M.; Meyerhoff, M. E. *Biomaterials* **2005**, *26*, 1685.
(30) Shin, J. H.; Schoenfisch, M. H. *Analyst* **2006**, *131*, 609.
(31) Shin, J. H.; Marxer, S. M.; Schoenfisch, M. H. *Anal. Chem.* **2004**, *76*, 4543.
(32) Marxer, S. M.; Rothrock, A. R.; Nablo, B. J.; Robbins, M. E.; Schoenfisch, M. H. *Chem. Mater.* **2003**, *15*, 4193.
(33) Robbins, M. E.; Oh, B. K.; Hopper, E. D.; Schoenfisch, M. H. *Chem. Mater.* **2005**, *17*, 3288.
(34) Frost, M. C.; Meyerhoff, M. E. *J. Biomed. Mater. Res., Part A* **2005**, *72A*, 409.
(35) Frost, M. C.; Meyerhoff, M. E. *J. Am. Chem. Soc.* **2004**, *126*, 1348.
(36) Nablo, B. J.; Schoenfisch, M. H. *Biomacromolecules* **2004**, *5*, 2034.
(37) Gallova, J.; Uhrikova, D.; Hanulova, M.; Teixeira, J.; Balgavy, P. *Colloids Surf., B* **2004**, *38*, 11.
(38) Zolkov, C.; Avnir, D.; Armon, R. *J. Mater. Chem.* **2004**, *14*, 2200.
(39) Jedlicka, S. S.; McKenzie, J. L.; Leavesley, S. J.; Little, K. M.; Webster, T. J.; Robinson, J. P.; Nivens, D. E.; Rickus, J. L. *J. Mater. Chem.* **2006**, *16*, 3221.
(40) Jedlicka, S. S.; Little, K. M.; Nivens, D. E.; Zemlyanov, D.; Rickus, J. L. *J. Mater. Chem.* **2007**, *17*, 5058.

(41) Zhelyaskov, V. R.; Gee, K. R.; Godwin, D. W. *Photochem. Photobiol.* **1998**, *67*, 282.

(42) Nguyen, T.; McNamara, K. P.; Rosenzweig, Z. *Anal. Chim. Acta* **1999**, *400*, 45.

(43) Padalkar, S.; Zhao, J.; Stuart, K.; Panitch, A.; Rickus, J.; Stanciu, L. *Ultramicroscopy* **2008**, *108*, 309.

(44) Stewart, J. C. M. *Anal. Biochem.* **1980**, *104*, 10.

(45) Porterfield, D. M.; Laskin, J. D.; Jung, S.-K.; Malchow, R. P.; Billack, B.; Smith, P. J. S.; Heck, D. E. *Am. J. Physiol. Lung Cell. Mol. Physiol.* **2001**, *281*, L904.

(46) Friedemann, M. N.; Robinson, S. W.; Gerhardt, G. A. *Anal. Chem.* **1996**, *68*, 2621.

(47) Porterfield, D. M. *Biosens. Bioelectron.* **2007**, *22*, 1186.

(48) Braun, S.; Rappoport, S.; Zusman, R.; Avnir, D.; Ottolenghi, M. *Mater. Lett.* **1990**, *10*, 1.

(49) Husing, N.; Reisler, E.; Zink, J. I. *J. Sol-Gel Sci. Technol.* **1999**, *15*, 57.

(50) Rickus, J. L.; Dunn, B.; Zink, J. I. Optically Based Sol-Gel Biosensor Materials. In *Optical Biosensors: Present and Future*; Ligler, F. S.; Rowe-Taitt, C. A., Eds.; Elsevier: Amsterdam, 2002; p 427.

(51) Rickus, J. L.; Chang, P. L.; Tobin, A. J.; Zink, J. I.; Dunn, B. *J. Phys. Chem. B* **2004**, *108*, 9325.

(52) Hope, M. J.; Bally, M. B.; Mayer, L. D.; Janoff, A. S.; Cullis, P. R. *Chem. Phys. Lipids* **1986**, *40*, 89.

(53) Kumar, S. M.; Porterfield, D. M.; Muller, K. J.; Smith, P. J. S.; Sahley, C. L. *J. Neurosci.* **2001**, *21*, 215.

(54) Nablo, B. J.; Schoenfisch, M. H. *Biomaterials* **2005**, *26*, 4405.

(55) Charville, G. W.; Hetrick, E. M.; Geer, C. B.; Schoenfisch, M. H. *Biomaterials* **2008**, *29*, 4039.

(56) Lancaster, J. R. *Proc. Natl. Acad. Sci. U.S.A.* **1994**, *91*, 8137.

JP803276U